Accepted Preprint first posted on 13 December 2016 as Manuscript JME-16-0200

Genetic characterization of a mouse line with primary aldosteronism

L.G. Perez-Rivas[1†], Y. Rhayem[1†], S. Sabrautzki[2,3], C. Hantel[1], B. Rathkolb[2,4,5], M. Hrabě de Angelis[2,4,6], M. Reincke[1], F. Beuschlein[1*], A. Spyroglou[1*]

[1]Medizinische Klinik und Poliklinik IV, Endocrine Research Unit, Klinikum der Universität München, LMU, Munich, Germany

[2]Helmholtz Zentrum München, German Research Center for Environmental Health (GmbH), Institute of Experimental Genetics and German Mouse Clinic, Ingolstädter Landstr.1, 85764 Neuherberg, Germany

[3]Helmholtz Zentrum München, German Research Center for Environmental Health (GmbH), Research Unit Comparative Medicine, Ingolstädter Landstr.1, 85764Neuherberg, Germany

[4]Member of German Center for Diabetes Research (DZD), Neuherberg, Germany

[5]Ludwig-Maximilians-Universität München, Chair for Molecular Animal Breeding and Biotechnology, Gene Center of the Ludwig-Maximilians-Universität München, Feodor-Lynen-Str. 25, 81377 München, Germany

[6]Lehrstuhl für Experimentelle Genetik, Technische Universität München, 85350 Freising-Weihenstephan, Germany

[†]L.G.-P.R. and Y.R. and [*]F.B. and A.S. equally contributed to this work

Correspondence and reprint request:

Felix Beuschlein, M.D.

Medizinische Klinik und Poliklinik IV, Endocrine Research Unit

Klinikum der Universität München

Ziemssenstr. 1, D-80336 Munich, Germany

p: xx49 (0)89 4400 52110, f: xx49 (0)89 4400 54467

e: felix.beuschlein@med.uni-muenchen.de

Short title: A mouse line with primary aldosteronism

Keywords: mutagenesis screen, primary aldosteronism, mouse model, steroidogenic enzymes

Word count: 4832

A mouse line with primary aldosteronism

Abstract

In an attempt to define novel genetic loci involved in the pathophysiology of primary aldosteronism a mutagenesis screen following treatment with the alkylating agent N-ethyl-N-nitrosourea was established for the parameter aldosterone. One of the generated mouse lines with hyperaldosteronism was phenotypically and genetically characterized. This mouse line had high aldosterone levels but normal creatinine and urea values. The steroidogenic enzyme expression levels in the adrenal gland did not differ significantly among phenotypically affected and unaffected mice. Upon exome sequencing point mutations were identified in seven candidate genes (*Sspo, Dguok, Hoxaas2, Clstn3, Atm, Tipin* and *Mapk6*). Subsequently, animals were stratified into wild-type and mutated groups according to their genotype for each of these candidate genes. A correlation of their genotypes with the respective aldosterone, aldosterone to renin ratio (ARR), urea, and creatinine values as well as steroidogenic enzyme expression levels was performed. Aldosterone values were significantly higher in animals carrying mutations in four different genes (*Sspo, Dguok, Hoxaas2* and *Clstn3*) and associated statistically significant adrenal *Cyp11b2* overexpression as well as increased ARR was present only in mice with *Sspo* mutation. In contrast, mutations of the remaining candidate genes (*Atm, Tipin* and *Mapk6*) were associated with lower aldosterone values and lower *Hsd3b6* expression levels. In summary, these data demonstrate association between the genes *Sspo, Dguok, Hoxaas2* and *Clstn3* and hyperaldosteronism. Final proofs for the causative nature of the mutations have to come from knock-out and knock-in experiments.

A mouse line with primary aldosteronism

Introduction

Arterial hypertension is a major cardiovascular risk factor affecting 30-45% of the adult European population (Mancia, et al. 2013) with primary aldosteronism being the most frequent cause of endocrine hypertension with a prevalence of 7-10% in unselected hypertensive patients (Hannemann, et al. 2012; Rossi, et al. 2006). The large majority of primary aldosteronism (PA) is caused either by an aldosterone producing adrenal adenoma or by bilateral adrenal hyperplasia (Mulatero, et al. 2004; Rossi et al. 2006). Despite its high prevalence, so far, the genetic causes of primary aldosteronism due to bilateral hyperplasia have been elucidated only in a very small subgroup of cases: Familial hyperaldosteronism type I is caused by unequal crossing-over of the *CYP11B1* and *CYP11B2* and the formation of a hybrid gene (Lifton, et al. 1992; Sutherland, et al. 1966), responsible for ACTH dependent production of aldosterone instead of being regulated by angiotensin II. Familial hyperaldosteronism type II (FH-2) seems also inherited as an autosomal dominant trait. A locus has been mapped on chromosome 7p22 in some but not all families (Gordon, et al. 1991; So, et al. 2005), but the linkage area has not been resolved to any causative mutation. Familial hyperaldosteronism type III (FH-3) (Geller, et al. 2008), however, has been recently linked to gain of function mutation in the *KCNJ5* gene, encoding an inwardly rectifying potassium channel (Choi, et al. 2011). These mutations induce a loss in channel selectivity, depolarization and increased intracellular Ca^{2+} concentrations leading to aldosterone excess. In a recent genetic analysis in 46 patients from 21 European families a new germline G151E mutation was identified (Mulatero, et al. 2012). *KCNJ5* mutations are more prevalent in females, younger patients, with higher aldosterone levels (Boulkroun, et al. 2012). Furthermore, exome sequencing in aldosterone producing adrenal adenomas revealed somatic mutations in *ATP1A1* and *ATP2A3*, two members of the P-type-ATPase gene family (Beuschlein, et al. 2013; Fernandes-Rosa, et al. 2014). Finally, germline mutations in the Ca^{2+}-channel genes *CACNA1D* (Scholl, et al. 2013) and *CACNA1H* (Scholl, et al. 2015) have been found as a rare cause of PA of early onset with *CACNA1D* mutations additionally causing neuromuscular abnormalities and partial or generalized seizures (Scholl et al. 2013). *CACNA1H* mutations were documented in patients with different phenotypic presentations of primary aldosteronism, such as early onset primary

aldosteronism, familial hyperaldosteronism or aldosterone producing adrenal adenoma (Daniil, et al. 2016). All in all, genetics of the vast majority of cases of bilateral adrenal hyperplasia remain enigmatic.

Animal models can play an important role in gaining functional insights into the physiology of aldosterone regulation and on the pathophysiology of autonomous aldosterone secretion. Furthermore they can be used for the investigation of cardiovascular effects of autonomous aldosterone synthesis on several organs and can serve for pharmacologic intervention studies. So far, though, only a few mouse models have been described with a phenotype reminiscent of primary aldosteronism. A mouse with TASK channel deletion (Davies, et al. 2008; Heitzmann, et al. 2008) and a circadian clock-deficient cry-null mouse model showing an upregulation of the adrenal *Hsd3b6* (Doi, et al. 2010) belong to this group. An approach to develop new mouse models for a specific phenotype is induction of genetic variation by random mutagenesis of the mouse genome using the mutagenic substance *N*-ethyl-*N*-nitrosourea (ENU) (Clark, et al. 2004; Hagge-Greenberg, et al. 2001; Hrabe de Angelis, et al. 2000). ENU is an alkylating agent that causes ethylation of nucleic acids and thereby point mutations in pre-meiotic spermatogonial stem cells (Rinchik 1991; Russell, et al. 1979). The mutations derived from ENU handling may, therefore, be hypomorph (partial loss-of-function). Mutants with gain-of-function as well as complete loss of function mutations are also possible (Justice, et al. 2000; Noveroske, et al. 2000). In the case of phenotype driven genetics the genomic association is accomplished utilizing common single nucleotide polymorphisms (SNPs) or more recently exome sequencing.

Objective of the present study was to phenotypically characterize a mouse line generated using this mutagenesis screen and to identify candidate genes correlating with the phenotype of primary aldosteronism.

Materials and methods

Animals and housing conditions

All animal studies were performed according to protocols examined and approved by the Regierung von Oberbayern and according to the German Animal Protection Law. Mice were kept in a specific pathogen-free animal facility area at an ambient temperature of 22±2°C, (relative humidity 60±5%) and on a 12h-12h light-dark circle. Animals were fed with chow #1314 (Altromin/Lage, Germany) ad libitum and had free access to tap water. C3HeB/FeJ mice (Jackson Laboratory, Bar Harbor, ME) involved in the experiments were maintained in groups of three or less individuals per cage. The generation of this mouse line with hyperaldosteronism has been described previously (Spyroglou, et al. 2011). In brief, in the Munich ENU project performed at the Institute of Experimental Genetics of the Helmholtz Center Munich, C3HeB/FeJ male mice were treated with three weekly injections of 90 mg/kg ENU at approximately 10-14 weeks of age. Recovery of fertility upon treatment could be observed approx. 80 days later. All F1 offspring from ENU-treated males and wild-type females born at least after two cycles of spermatogenesis following the last injection were checked for their aldosterone levels in plasma at the age of 12 and 16 weeks. Out of this cohort of 2800 offspring, 83 displayed high aldosterone values at the age of 12 weeks and upon confirmation measurement at the age of 16 weeks only 11 mice had sustained high aldosterone values (2 males and 9 females). Upon mating to wild-type mice eight lines with affected offspring in the heterozygous state had been established. Here we describe the phenotypical and genetic characterization of one of these mouse lines.

Blood sampling

To avoid any influence of the examined parameters through hypothalamic-pituitary-adrenal (HPA) axis activation, handling of the animals until blood sampling was kept to an interval of less than one minute. Blood sampling took place between 8:00 and 11:00 am for all animals. After effective inhalation anesthesia, the retro-bulbar vein plexus of the mouse was punctured with a glass capillary (external diameter 0.8 mm) and from each animal blood was collected in Li-Heparin coated tubes to

avoid coagulation. After centrifugation (10000g, 10min) plasma was separated and kept at -20°C until measurement.

Biochemical and endocrine profiling

Urea and creatinine values were measured in the clinical chemical laboratory of the German Mouse Clinic (Fuchs, et al. 2011) using an AU480 Autoanalyser (Beckman-Coulter/Krefeld, Germany) and adapted reagent kits provided by the manufacturer (Urea: OSR6134; creatinine (Jaffe): OSR6178)(Rathkolb, et al. 2013).

Aldosterone was determined in 50 µl of mouse plasma samples with an in-house time resolved fluorescent immunoassay as described in detail elsewhere (Manolopoulou, et al. 2008).

After 1.5 hrs of incubation of two equal fractions of each mouse plasma sample with plasma of bilaterally nephrectomized male rats as renin substrate at 0°C and 37°C, respectively (pH=6, with addition of the protease inhibitor PMSF), angiotensin I was generated. Subsequently, angiotensin I concentration of each fraction was measured by a commercially available Angiotensin I (PRA) ELISA Kit (IBL international, Hamburg, Germany) according to the manufacturer's instructions. Plasma renin activity in each sample was calculated using the following equation: PRA= [(AngI 37°C – AngI 0°C)/incubation time (hrs)]*1.11. Aldosterone to renin ratios (ARR) were calculated for each mouse sample and expressed as % of the mean of male or female wild-types, respectively.

Corticosterone levels were measured with the Corticosterone HS EIA Immunoassay (IDS, Boldon, Tyne and Wear, United Kingdom) according to the manufacturers' instructions.

Organ sampling

Following anesthesia, mice were euthanized and the abdominal cavity was opened. Both adrenal glands of each mouse, as well as the spleen were identified and removed. Directly after collection, adrenals were cleaned from surrounding fat tissue using a stereoscope. All organs were snap frozen in liquid nitrogen and stored in -80°C or stored in 4% paraformaldehyde and subsequently embedded in paraffin blocks.

158 *Capture and sequencing of murine exomes*

159 In-solution targeted enrichment of exonic sequences was performed by DNA extracted from the
160 spleens of two different affected animals from the first and third generation respectively by using the
161 SureSelectXT Mouse All Exon 50 Mb kit from Agilent (Santa Clara, CA, USA) as already described
162 (Diener, et al. 2016). The generated libraries were indexed, pooled, and sequenced as 100 bp paired-
163 end runs on a HiSeq2000 system (Illumina, San Diego, CA, USA).

164

165 *Mapping and variant calling*

166 Read alignment to the mouse genome assembly mm9 was done with Burrows–Wheeler Aligner
167 (BWA, version 0.6.2) and yielded 12.1 and 11.5 Gb of mapped sequence data corresponding to an
168 average coverage of 143x and 137x respectively. Single-nucleotide variants (SNVs) and small
169 insertions and deletions (indels) were detected with SAMtools (version 0.1.18). SNVs were only
170 lightly filtered on quality scores (SNV quality >40, mapping quality >50), because we preferred false
171 positives to negatives. After subtracting variants from dbSNP128, and from 158 other mice in our in-
172 house database, 31 unique coding variants specific to the mutant mouse line remained.

173

174 *Validation of candidate variants by capillary Sanger sequencing*

175 Candidate SNVs were further investigated by amplifying DNA of mutant and control mice with
176 intronic primers (Supplemental Table 1). Bidirectional Sanger sequencing was then performed using
177 the ABI Prism BigDye Terminator v.3.1 Cycle Sequencing Kit on an ABI Prism 3700 DNA Analyzer
178 (Applied Biosystems, ThermoFischerScientific, Waltham, USA). A genotype-phenotype correlation
179 was then performed.

180

181 *Real-Time PCR*

182 Both adrenals from each individual animal were combined and homogenized in extraction buffer
183 while still frozen. RNA extraction was performed using the Maxwell 16 LEV simplyRNA according
184 to the manufacturer's instructions (Promega, Mannheim, Germany). RNA quantification was
185 performed with the Nanodrop spectrophotometer. The 260/280-absorbance ratio was used to assess

RNA purity. Additionally, RNA integrity was assessed on denaturing agarose gel stained with ethidium bromide. For cDNA synthesis, 500ng of total RNA were reverse transcribed according to the manufacturers' instructions (M-MLV Reverse Transcriptase, dNTP Mix, Recombinant RNasin Ribonuclease Inhibitor all from Promega, Mannheim, Germany). The expression of selected genes involved in steroidogenesis was investigated: *StAR* (Steroidogenic acute regulatory protein), *Cyp11a1* (cholesterol side-chain cleavage enzyme), *Hsd3b6* (3β-hydroxysteroid dehydrogenase), *Cyp11b1* (11β-hydroxylase), *Cyp11b2* (aldosterone synthase), *Nurr1*, *Nur77*, *Kim1* (Kidney injury molecule-1, Havcr1). *Gapdh* was used as reference gene. For primer sequences see Supplemental table 1. The SsoFast EVAGreen Supermix (Biorad Laboratories Berkley, CA) in the Mx3000P QPCR System (Stratagene, La Jolla, CA) was used for the quantification of the investigated genes. Real-time PCR conditions in the Mx3000P are as indicated in Supplemental Table 1.To verify the presence of a unique amplicon with the correct size, a melting curve analysis was performed between 55°and 95°C (0.1° C/sec) and the products were run on a 1% agarose gel. To proof the specificity of the amplification product for each primer pair, we performed sequencing of the different genes with the primers used for the qPCR experiments. Quantification was adjusted using the mouse *Gapdh* expression as reference. With a coefficient of variation (CV) below 5%, *Gapdh* was considered having a stable expression in the adrenal gland and therefore was chosen to be used as housekeeping gene in this experimental setting.

Histological Examination

Tissues remained in 4% paraformaldehyde overnight and then were dehydrated, embedded in paraffin, sectioned, and stained with hematoxylin and eosin following standard protocols. Hematoxylin and eosin–stained adrenal sections were examined with a light microscope using magnifications of x40 and x400.

For CYP11B2 immunohistochemistry, paraffin-embedded sections were rehydrated, blocked with 0.3% H_2O_2 in methanol for 10 min, and incubated with blocking buffer (0.1M Tris-HCl pH=7.4 (Sigma-Aldrich, Taufkirchen, Germany), 20% goat serum (Jackson ImmunoResearch Laboratories, West Grove, PA, USA), 0.05% SDS (Sigma-Aldrich)) for 1 hr. CYP11B2 was immunodetected

overnight at 4°C by means of a rabbit-anti-mouse-CYP11B2 antibody (kindly provided by Prof. Celso Gomez-Sanchez, University of Mississippi, USA) in a dilution of 1:1000 in an antibody buffer containing 0.1M Tris-HCl, 20% goat serum, and 0.1% Tween 20 (Sigma-Aldrich). After rinsing for 15 min in PBS, secondary antibody (goat-anti-rabbit-biotinylated IgG (Vector Laboratories, Burlingame, CA, USA)) in a dilution of 1:2000 in antibody buffer was applied for 30 min at room temperature. For the visualization of the bound CYP11B2 antibody, Vectastain Elite ABC system (Vector Laboratories) and Sigma Fast diaminobenzidine (Sigma-Aldrich) were used and slides were counterstained with Harry's haematoxylin.

All captured images were color-calibrated to the negative control. A randomly selected rectangle area of the adrenal cortex of each animal extending vertically from the outer border of the adrenal medulla up to the surface of the adrenal gland was divided into three subareas (outer (1/4), middle (2/4) and inner area (1/4)). The total counterstained cell population of the selected area was analyzed according to the color of the cell cytoplasm; cells were categorized as positive or negative. Positively and negatively CYP11B2 - stained cells were counted on three independent sections per animal by two independent investigators under blinded conditions. Results are presented as means of ratios of positive to total cell counts per standardized area.

Statistical analysis

Statistical analysis was carried out with the Prism 3.02 (GraphPad Software, La Jolla, USA). Statistical significance was determined using the unpaired t-test for normally distributed parameters and Mann-Whitney test for non-normally distributed parameters. Statistical significance was denoted by asterisks in the figures as *$P<0.05$, **$P<0.01$, and ***$P<0.001$.

Results

Screening parameters

All offspring of the founder animal (n=158, Figure 1) were tested for their aldosterone values at the age of 12 and 16 weeks. Animals repeatedly showing increased values were grouped to the "affected group" and those with normal values (normal rage: mean ± 3 standard deviations, defined previously (Spyroglou et al. 2011)) to the "unaffected group". Out of this cohort 33 animals (17 unaffected, 16 affected) from generations F3-5 were further analyzed. As expected, affected animals of both genders had significantly higher aldosterone values than their unaffected littermates ($P<0.001$, Figure 2A, 33% of all offspring of this mouse line were affected and the affected male: female ratio was 4:3). Corticosterone levels of affected and unaffected animals of both genders did not differ significantly (unaffected: 2.64 ±1.5ng/ml, affected 2.36±1.79 ng/ml, $P=0.75$), and no correlation of aldosterone to corticosterone values could be observed ($R=0.16$, $P=0.52$), excluding increased stress as confounding factor for the elevated aldosterone values. Urea and creatinine, as parameters of kidney function, showed no differences between affected animals and their unaffected littermates, suggesting that secondary hyperaldosteronism due to overt renal disease can be excluded in this mouse line (Figure 2B and C).Consistently, the expression of *Kim1,* as a biomarker of renal tubule injury, did not differ in the two groups (relative expression normalized to *Gapdh*: unaffected: 0.08884 ± 0.01548, affected: 0.1163 ± 0.03992, $P=0.46$).

Expression levels of several genes involved in steroidogenesis were quantified in the adrenal glands of these animals. Unexpectedly, the expression levels of all investigated steroidogenic enzymes (*StAR, Cyp11a1, Hsd3b6, Cyp11b1* and *Cyp11b2*) and orphan nuclear factors (*Nurr1* and *Nur77*-data not shown) did not display any statistically significant differences between unaffected and affected animals (Figure 2D-I).

Identified candidate genes

For the genotypic characterization of the mouse line we made use of *Next Generation Sequencing* (NGS) exome analysis (Institute of Human Genetics, Helmholtz Center Munich, (Diener et al. 2016)).

A mouse line with primary aldosteronism

After exome sequencing performed on two different affected animals from the first and third generation respectively, a list with induced single nucleotide variations (SNV), filtered on the basis of technical quality criteria (SNV quality >40, mapping quality > 50) was generated (supplemental Table 2). Exome sequencing identified SNVs on 31 different genes; eight of those were common for both investigated animals: SCO-spondin (*Sspo*), deoxyguanosine kinase (*Dguok*), 5730446D14Rik (Hoxa cluster antisense RNA 2 – *Hoxaas2*), calsyntenin 3 (*Clstn3*), integrator complex subunit 10 (*Ints10*), ataxia telangiectasia mutated (*Atm*), timeless interacting protein (*Tipin*), mitogen-activated protein kinase 6 (*Mapk6*).*Sspo*, *Dguok*, *Hoxaas2* and *Clstn3*are located on mouse chromosome 6, *Ints10*is located on chromosome 8 and *Atm*, *Tipin* and *Mapk6* are located on chromosome 9. These were subsequently sequenced in a large cohort (n=126, 63 females, 63 males) of phenotypically "affected" and "unaffected" animals of this mouse line. Ints10 was not found mutated in the examined cohort of animals and was excluded from further analyses. Since ENU is likely to induce more coding SNVs in the first generations than the one responsible for the 'high aldosterone' phenotype we again investigated the potential function of those genes and their expression levels in the adrenal gland. Based on a detailed database search, none of the genes had a known function in the adrenal gland and/or aldosterone biosynthesis. Increased adrenal expression according to the BioGPS database could be documented only for the murine *Clstn3* gene.

Genotype / phenotype correlation

In an attempt to correlate the identified candidate genes with the phenotype of interest, animals were stratified into wild-type and mutated groups according to their genotypes for each of the candidate genes. We correlated the genotype with the respective aldosterone, urea, and creatinine values as well as steroidogenic enzyme expression levels. In order to uniformly assess differences in the aldosterone values in mice of both genders these were expressed as percentage of the mean of the respective gender. Due to the fact that the majority of investigated animals carried more than one of the seven SNVs identified during the study, for the results depicted in Figure 3 and 4 animals carrying two wild type copies for the respective gene were considered as "wild types". Thus, in the majority of cases these animals were carriers of mutant variants of one or several genes of the panel. Along the same

line, "mutants" for the specific gene often also carried in parallel further mutations. Thereby, we aimed at isolating a potential effect of one mutation on the investigated phenotype even though the random presence of other variants might have further modulating effects. We observed significantly increased plasma aldosterone values in animals carrying an *Sspo* (P<0.01), *Dguok* (P<0.01), *Hoxaas2* (P<0.01) and *Clstn3* (P<0.001) mutation. In contrast, animals carrying the wild-type gene for *Atm*, *Tipin* and *Mapk6* displayed significantly higher aldosterone values than their mutant littermates (Figure 3). Urea and creatinine levels did not differ significantly among wild-type and mutated animals.

The correlation of the expression levels of steroidogenic enzymes to the genotypes was less clear-cut with large variation among wild-type and mutated animals in most of the cases. StAR expression levels, regulating the initial step in steroidogenesis, were significantly lower in *Clstn3* mutated animals (P<0.05, Figure 4A), whereas Cyp11a1 expression was lowered in *Sspo* (p<0.05), *Dguok* (P<0.01), *Hoxaas2* (P<0.01), *Clstn3* (P<0.001) and *Atm* (P<0.05) mutants (Figure 4B). Significantly lower were also the Hsd3b6 levels in *Clstn3* (P<0.05), *Atm* (P<0.01), *Tipin* (P<0.05) and *Mapk6* (P<0.05) mutated animals (Figure 4C). No such differences could be found for Cyp11b1 expression levels for any of the mutations investigated (Figure 4D). In *Sspo* mutated animals Cyp11b2 expression, as marker of the rate limiting step of aldosterone biosynthesis, was significantly higher (P<0.05). *Dguok* mutated animals showed a tendency to higher Cyp11b2 levels, without reaching statistical significance (P=0.07), (Figure 4E).The orphan nuclear factor Nurr1, also involved in the aldosterone synthesis was found significantly higher in *Sspo* (P<0.05) and *Hoxaas2* (P<0.05) mutated mice. *Dguok* mutants also tended to display higher Nurr1 levels (P=0.08), (Figure 4F).

From the results depicted in Figure 3 we conclude that *Atm*, *Tipin* and *Mapk6* do not correlate with the phenotype of primary aldosteronism, since aldosterone values in wild-type animals were found significantly higher than in animals carrying one, two or all three SNVs. To further narrow down our list to one causative SNV from the remaining four genes (*Sspo, Dguok, Hoxaas2* and *Clstn3*), we compared aldosterone levels of animals excluding mice carrying *Atm* and/or *Tipin* and/or *Mapk6* mutations. Animals carrying *Sspo* and/or *Dguok* and/or *Hoxaas2* and/or *Clstn3* SNVs displayed significantly higher aldosterone values than wild-type only animals and the mutant to wild-type ratio

was in all cases higher in this restricted analysis (Table 1, for detailed combination of the variants see Supplemental Table 3). A combination of SNVs in both chromosomes 6 and 9 (all seven mutations) lead to weakening of the phenotype of hyperaldosteronism (data not shown).

Quantification of plasma renin activity in these animals did not present any significant differences between animals with wild-type and mutant genotype for the above four SNVs. Calculation of the aldosterone to renin ratios (ARR) showed a significant ARR increase only in mice carrying the *Sspo* SNV (Table 2). Mice with the *Dguok* and/or *Hoxaas2* SNV presented a tendency towards increased ARRs.

Interestingly, when comparing corticosterone levels of animals carrying the four different mutations to their wild-type littermates it could be observed that mutant animals displayed slightly lower corticosterone values than the wild-types without reaching statistical significance (mutants: 2.36 ± 0.53 ng/ml vs. wild-types: 4.06 ± 0.95 ng/ml, P=0.14).

Histological examination of the adrenal glands of animals carrying all four SNVs (*Sspo, Dguok, Hoxaas2* and *Clstn3*) did not reveal any adrenocortical adenomas. Moreover, there was no indication of hyperplasia, since the cell count of the outer, middle and inner cortical area of these animals did not differ significantly from the wild-types (P=0.45, P=0.80 and P=0.29, respectively). However, immunohistochemical staining with murine CYP11B2 antibody showed significantly more positively stained cells in the adrenal cortex of mutant animals in comparison to the wild-types (P<0.001, Figure 5A-C). Additionally, in the adrenal cortex of mutant animals CYP11B2 staining was significantly more pronounced in the middle (P<0.001) and inner (P<0.001) area when compared to wild-types, suggesting an alternated zonation pattern in animals carrying the four SNVs (Figure 5D-F). Thereby, the presence of aldosterone synthase expression in the middle and inner cortical area of the mutant animals seems to exclusively account for the increased total expression of aldosterone synthase.

Discussion

In this study, an ENU-mutagenesis derived mouse line with hyperaldosteronism was phenotypically and genetically characterized. The trait of increased aldosterone values above 3 standard deviations from the mean was preserved for more than five generations in a considerable proportion of animals of both genders. Specifically, one third of all investigated animals were affected, with the ratio of males to females being 4:3. Animals with high aldosterone values showed in all cases normal kidney retention parameters and *Kim1* expression excluding a relevant renal disorder as the cause for the described phenotype. Furthermore, corticosterone levels, mirroring stress levels of affected and unaffected animals did not differ in the present study. However, the adrenal expression of steroidogenic enzymes and especially *Cyp11b2*, the rate limiting step of aldosterone biosynthesis was not concordant with the significantly increased plasma aldosterone levels. Although blood pressure measurement would have been a clinically relevant endpoint in the investigation of this mouse model in the context of the current study, we focused on the adrenal phenotype of these animals. Future investigations with state-of-the-art analytic methods will be required to investigate in depth the cardiovascular effects of the animal model.

Following the described approach, we identified seven candidate genes for the phenotype hyperaldosteronism. Out of the identified genes none had a known function in aldosterone secretion or regulation and only *Clstn3* had a pronounced expression in the mouse adrenal gland as well as in the pituitary and brown adipose tissue according to the BioGPS database. *Clstn3* codes for a postsynaptic Ca^{2+} binding-membrane protein, a member of the cadherin superfamily involved in the development of synapses (Lu, et al. 2014), with highest expression levels in GABAergic neurons (Hintsch, et al. 2002). It is also present in endocrine secretory granules of gonadotrope, somatotrope and thyrotrope cells of the anterior pituitary, whereas Clstn1, another member of the superfamily, was found to be localized in glucagon-containing secretory granules of pancreatic α-cells (Rindler, et al. 2008). Thus, it is hypothesized that soluble Clstns, released locally, could potentially serve as modulators of endocrine function (Rindler et al. 2008). Although *Clstn3* has not been appreciated to play a functional role in adrenal physiology or disease it is the strength of a hypothesis free approach such as the ENU screen that potentially surprising findings can be generated. Exome sequencing from patient samples

(Beuschlein et al. 2013; Beuschlein, et al. 2014) and population based genetic studies (Spyroglou, et al. 2014) provide examples for the power of these strategies.

When aldosterone values were displayed with mice grouped according to the presence or absence of specific mutations, an interesting phenomenon was observed: Animals carrying part of the identified mutations displayed significantly lower aldosterone levels compared to the wild-types for the specific mutation. An explanation for this paradoxical finding could be that animals were misleadingly grouped into "mutant" and "wild-types" for the specific genes, since these genotypes were not responsible for the phenotype of interest. Accordingly, *Atm, Tipin* and *Mapk6*, all located on chromosome 9 and apparently inherited in parallel, probably due to genetic linkage, seem not to be causative for the hyperaldosteronism phenotype, since aldosterone values of "wild-type" animals were in these three cases higher than in their "mutant" littermates. In contrast, it was reassuring that SNVs on *Sspo, Dguok, Hoxaas2* and *Clstn3*, all located on chromosome 6 were associated with a significant increase in aldosterone values of the respective mutant animals, suggesting a role of these genes in the phenotype of primary aldosteronism. Upon calculation of the aldosterone to renin ratio, only animals with the *Sspo* SNV showed higher ARRs in comparison to their wild-type littermates, suggesting possibly a particular role of this gene in the described phenotype.

Furthermore, it can be speculated that downregulation of the initial enzymes of steroidogenesis, such as StAR, Cyp11a1 and Hsd3b6 as displayed on Figure 4 was due to a negative feedback loop by parallel autonomous aldosterone secretion. Consistent with the unchanged *Cyp11b1* expression, no differences in corticosterone values could be observed in the study. Additionally, we observe a discrepancy between the moderate adrenal *Cyp11b2* RNA expression and the significantly higher aldosterone values, aldosterone to renin ratios and number of CYP11B2 positively-stained adrenocortical cells in mutant animals. The interpretation of the only mild *Cyp11b2* upregulation with presence of SNVs on some of the investigated genes (*Sspo* and much less *Dguok*), or complete absence of upregulation in other cases (*Hoxaas2, Clstn3*) appears thereby more challenging. However, it is possible that even moderate increased *Cyp11b2* RNA expression could result in a pronounced difference in protein expression possibly due to increased stability of this enzyme. This explanation would require further analysis. Another interesting observation in mutant animals (all four *Sspo,*

Dguok, Hoxaas2 and *Clstn3*) is that the increase in aldosterone synthase expression seems to base on the presence of aldosterone synthase expression in the middle and inner adrenocortical area. This alteration of the functional zonation of the adrenal cortex also needs further elucidation.

Taken together, from the identified candidate genes *Atm, Tipin* and *Mapk6* seem to not be responsible for the investigated phenotype of primary aldosteronism, whereas no safe conclusion can be conducted in the case of *Sspo, Dguok, Hoxaas2* and *Clstn3* and their potential role in PA. Ideally, to distinguish among those four genes, further breeding should take place in order to genetically separate them in strains carrying only one candidate SNV. Practically, this was not yet achieved after seven generations of breeding following embryotransfer (F1-F7), probably since all four genes are located in near regions of the same chromosome and thereby inherited together. Thus, further efforts will be necessary to rule in or out the role of these four genes in the pathogenesis of primary aldosteronism.

412 **Declaration of Interest**

413 The authors declare that there is no conflict of interest that could be perceived as prejudicing the
414 impartiality of the research reported.

415

416 **Funding**

417 This work was supported by a grant from the Deutsche Hochdruckliga and in part by a grant from the
418 Bayerische Gleichstellungsförderung to A.S. and funds from the People Programme (Marie Curie
419 Actions) of the European Union's Seventh Framework Programme (FP7/2007-2013) under REA grant
420 agreement n^{o} 608 765 to LGP-R.

421

422 **Acknowledgment**

423 The authors are indebted to Brigitte Mauracher, Sebastian Kaidel, Andreas Mayer and Sandra
424 Hoffmann for excellent technical assistance.

425

426

References

Beuschlein F, Boulkroun S, Osswald A, Wieland T, Nielsen HN, Lichtenauer UD, Penton D, Schack VR, Amar L, Fischer E, et al. 2013 Somatic mutations in ATP1A1 and ATP2B3 lead to aldosterone-producing adenomas and secondary hypertension. *Nat Genet* **45** 440-444, 444e441-442.

Beuschlein F, Fassnacht M, Assie G, Calebiro D, Stratakis CA, Osswald A, Ronchi CL, Wieland T, Sbiera S, Faucz FR, et al. 2014 Constitutive activation of PKA catalytic subunit in adrenal Cushing's syndrome. *N Engl J Med* **370** 1019-1028.

Boulkroun S, Beuschlein F, Rossi GP, Golib-Dzib JF, Fischer E, Amar L, Mulatero P, Samson-Couterie B, Hahner S, Quinkler M, et al. 2012 Prevalence, clinical, and molecular correlates of KCNJ5 mutations in primary aldosteronism. *Hypertension* **59** 592-598.

Choi M, Scholl UI, Yue P, Bjorklund P, Zhao B, Nelson-Williams C, Ji W, Cho Y, Patel A, Men CJ, et al. 2011 K+ channel mutations in adrenal aldosterone-producing adenomas and hereditary hypertension. *Science* **331** 768-772.

Clark AT, Goldowitz D, Takahashi JS, Vitaterna MH, Siepka SM, Peters LL, Frankel WN, Carlson GA, Rossant J, Nadeau JH, et al. 2004 Implementing large-scale ENU mutagenesis screens in North America. *Genetica* **122** 51-64.

Daniil G, Fernandes-Rosa FL, Chemin J, Blesneac I, Beltrand J, Polak M, Jeunemaitre X, Boulkroun S, Amar L, Strom TM, et al. 2016 CACNA1H Mutations Are Associated With Different Forms of Primary Aldosteronism. *EBioMedicine*.

Davies LA, Hu C, Guagliardo NA, Sen N, Chen X, Talley EM, Carey RM, Bayliss DA & Barrett PQ 2008 TASK channel deletion in mice causes primary hyperaldosteronism. *Proc Natl Acad Sci U S A* **105** 2203-2208.

Diener S, Bayer S, Sabrautzki S, Wieland T, Mentrup B, Przemeck GK, Rathkolb B, Graf E, Hans W, Fuchs H, et al. 2016 Exome sequencing identifies a nonsense mutation in Fam46a associated with bone abnormalities in a new mouse model for skeletal dysplasia. *Mamm Genome*.

Doi M, Takahashi Y, Komatsu R, Yamazaki F, Yamada H, Haraguchi S, Emoto N, Okuno Y, Tsujimoto G, Kanematsu A, et al. 2010 Salt-sensitive hypertension in circadian clock-deficient Cry-null mice involves dysregulated adrenal Hsd3b6. *Nat Med* **16** 67-74.

Fernandes-Rosa FL, Williams TA, Riester A, Steichen O, Beuschlein F, Boulkroun S, Strom TM, Monticone S, Amar L, Meatchi T, et al. 2014 Genetic spectrum and clinical correlates of somatic mutations in aldosterone-producing adenoma. *Hypertension* **64** 354-361.

Fuchs H, Gailus-Durner V, Adler T, Aguilar-Pimentel JA, Becker L, Calzada-Wack J, Da Silva-Buttkus P, Neff F, Gotz A, Hans W, et al. 2011 Mouse phenotyping. *Methods* **53** 120-135.

Geller DS, Zhang J, Wisgerhof MV, Shackleton C, Kashgarian M & Lifton RP 2008 A novel form of human mendelian hypertension featuring nonglucocorticoid-remediable aldosteronism. *J Clin Endocrinol Metab* **93** 3117-3123.

Gordon RD, Stowasser M, Tunny TJ, Klemm SA, Finn WL & Krek AL 1991 Clinical and pathological diversity of primary aldosteronism, including a new familial variety. *Clin Exp Pharmacol Physiol* **18** 283-286.

Hagge-Greenberg A, Snow P & O'Brien TP 2001 Establishing an ENU mutagenesis screen for the piebald region of mouse Chromosome 14. *Mamm Genome* **12** 938-941.

Hannemann A, Bidlingmaier M, Friedrich N, Manolopoulou J, Spyroglou A, Volzke H, Beuschlein F, Seissler J, Rettig R, Felix SB, et al. 2012 Screening for primary aldosteronism in hypertensive subjects: results from two German epidemiological studies. *Eur J Endocrinol* **167** 7-15.

475 Heitzmann D, Derand R, Jungbauer S, Bandulik S, Sterner C, Schweda F, El Wakil A, Lalli
476 E, Guy N, Mengual R, et al. 2008 Invalidation of TASK1 potassium channels disrupts adrenal
477 gland zonation and mineralocorticoid homeostasis. *Embo J* **27** 179-187.
478 Hintsch G, Zurlinden A, Meskenaite V, Steuble M, Fink-Widmer K, Kinter J & Sonderegger
479 P 2002 The calsyntenins--a family of postsynaptic membrane proteins with distinct neuronal
480 expression patterns. *Mol Cell Neurosci* **21** 393-409.
481 Hrabe de Angelis MH, Flaswinkel H, Fuchs H, Rathkolb B, Soewarto D, Marschall S,
482 Heffner S, Pargent W, Wuensch K, Jung M, et al. 2000 Genome-wide, large-scale production
483 of mutant mice by ENU mutagenesis. *Nat Genet* **25** 444-447.
484 Justice MJ, Carpenter DA, Favor J, Neuhauser-Klaus A, Hrabe de Angelis M, Soewarto D,
485 Moser A, Cordes S, Miller D, Chapman V, et al. 2000 Effects of ENU dosage on mouse
486 strains. *Mamm Genome* **11** 484-488.
487 Lifton RP, Dluhy RG, Powers M, Rich GM, Cook S, Ulick S & Lalouel JM 1992 A chimaeric
488 11 beta-hydroxylase/aldosterone synthase gene causes glucocorticoid-remediable
489 aldosteronism and human hypertension. *Nature* **355** 262-265.
490 Lu Z, Wang Y, Chen F, Tong H, Reddy MV, Luo L, Seshadrinathan S, Zhang L, Holthauzen
491 LM, Craig AM, et al. 2014 Calsyntenin-3 molecular architecture and interaction with
492 neurexin 1alpha. *J Biol Chem* **289** 34530-34542.
493 Mancia G, Fagard R, Narkiewicz K, Redon J, Zanchetti A, Bohm M, Christiaens T, Cifkova
494 R, De Backer G, Dominiczak A, et al. 2013 2013 ESH/ESC Guidelines for the management
495 of arterial hypertension: the Task Force for the management of arterial hypertension of the
496 European Society of Hypertension (ESH) and of the European Society of Cardiology (ESC). *J*
497 *Hypertens* **31** 1281-1357.
498 Manolopoulou J, Bielohuby M, Caton SJ, Gomez-Sanchez CE, Renner-Mueller I, Wolf E,
499 Lichtenauer UD, Beuschlein F, Hoeflich A & Bidlingmaier M 2008 A highly sensitive
500 immunofluorometric assay for the measurement of aldosterone in small sample volumes:
501 validation in mouse serum. *J Endocrinol* **196** 215-224.
502 Mulatero P, Stowasser M, Loh KC, Fardella CE, Gordon RD, Mosso L, Gomez-Sanchez CE,
503 Veglio F & Young WF, Jr. 2004 Increased diagnosis of primary aldosteronism, including
504 surgically correctable forms, in centers from five continents. *J Clin Endocrinol Metab* **89**
505 1045-1050.
506 Mulatero P, Tauber P, Zennaro MC, Monticone S, Lang K, Beuschlein F, Fischer E, Tizzani
507 D, Pallauf A, Viola A, et al. 2012 KCNJ5 mutations in European families with
508 nonglucocorticoid remediable familial hyperaldosteronism. *Hypertension* **59** 235-240.
509 Noveroske JK, Weber JS & Justice MJ 2000 The mutagenic action of N-ethyl-N-nitrosourea
510 in the mouse. *Mamm Genome* **11** 478-483.
511 Rathkolb B, Hans W, Prehn C, Fuchs H, Gailus-Durner V, Aigner B, Adamski J, Wolf E &
512 Hrabe de Angelis M 2013 Clinical Chemistry and Other Laboratory Tests on Mouse Plasma
513 or Serum. *Curr Protoc Mouse Biol* **3** 69-100.
514 Rinchik EM 1991 Chemical mutagenesis and fine-structure functional analysis of the mouse
515 genome. *Trends Genet* **7** 15-21.
516 Rindler MJ, Xu CF, Gumper I, Cen C, Sonderegger P & Neubert TA 2008 Calsyntenins are
517 secretory granule proteins in anterior pituitary gland and pancreatic islet alpha cells. *J*
518 *Histochem Cytochem* **56** 381-388.
519 Rossi GP, Bernini G, Caliumi C, Desideri G, Fabris B, Ferri C, Ganzaroli C, Giacchetti G,
520 Letizia C, Maccario M, et al. 2006 A prospective study of the prevalence of primary
521 aldosteronism in 1,125 hypertensive patients. *J Am Coll Cardiol* **48** 2293-2300.
522 Russell WL, Kelly EM, Hunsicker PR, Bangham JW, Maddux SC & Phipps EL 1979
523 Specific-locus test shows ethylnitrosourea to be the most potent mutagen in the mouse. *Proc*
524 *Natl Acad Sci U S A* **76** 5818-5819.

525 Scholl UI, Goh G, Stolting G, de Oliveira RC, Choi M, Overton JD, Fonseca AL, Korah R,
526 Starker LF, Kunstman JW, et al. 2013 Somatic and germline CACNA1D calcium channel
527 mutations in aldosterone-producing adenomas and primary aldosteronism. *Nat Genet* **45**
528 1050-1054.
529 Scholl UI, Stolting G, Nelson-Williams C, Vichot AA, Choi M, Loring E, Prasad ML, Goh G,
530 Carling T, Juhlin CC, et al. 2015 Recurrent gain of function mutation in calcium channel
531 CACNA1H causes early-onset hypertension with primary aldosteronism. *Elife* **4** e06315.
532 So A, Duffy DL, Gordon RD, Jeske YW, Lin-Su K, New MI & Stowasser M 2005 Familial
533 hyperaldosteronism type II is linked to the chromosome 7p22 region but also shows predicted
534 heterogeneity. *J Hypertens* **23** 1477-1484.
535 Spyroglou A, Bozoglu T, Rawal R, De Leonardis F, Sterner C, Boulkroun S, Benecke AG,
536 Monti L, Zennaro MC, Petersen AK, et al. 2014 Diastrophic dysplasia sulfate transporter
537 (SLC26A2) is expressed in the adrenal cortex and regulates aldosterone secretion.
538 *Hypertension* **63** 1102-1109.
539 Spyroglou A, Wagner S, Gomez-Sanchez C, Rathkolb B, Wolf E, Manolopoulou J, Reincke
540 M, Bidlingmaier M, Hrabe de Angelis M & Beuschlein F 2011 Utilization of a mutagenesis
541 screen to generate mouse models of hyperaldosteronism. *Endocrinology* **152** 326-331.
542 Sutherland DJ, Ruse JL & Laidlaw JC 1966 Hypertension, increased aldosterone secretion
543 and low plasma renin activity relieved by dexamethasone. *Can Med Assoc J* **95** 1109-1119.
544
545

546

A mouse line with primary aldosteronism

Table and Figure legends:

Table 1: Aldosterone plasma levels (pg/ml, mean ± SD) in animals with the respective genotype in the whole cohort (all) and excluding animals with mutations in Atm, Tipin, and/or Makp6 (restricted).

Table 2: Aldosterone to Renin Ratio of all experimental animals. In each line "mut" denotes those mice which carry at least the respective mutant gene while "wt" combine those with absence of the mutant gene.

Figure 1: Pedigree of the investigated mouse line with primary aldosteronism. Increased aldosterone values (+3 SD from the mean) observed in five successive generations, in animals of both genders. Affected animals 33%, males: females ratio 4:3. Squares: males, circles: females, black: affected animals.

Figure 2: (A) Aldosterone values in affected mice (n=16), significantly higher than in their unaffected littermates (n=17, $P<0.001$). No differences in creatinine and urea values in affected and unaffected animals (B, C). No differences in the expression levels of the steroidogenic enzymes leading to aldosterone production (D-I).

Figure 3: Aldosterone values in wild-type or mutant animals (n=126) for each of the following genes: *Sspo, Dguok, Hoxaas2, Clstn3, Atm, Tipin* and *Mapk6*. Values are expressed as % of the mean aldosterone levels of wild-type male or female mice respectively.

Figure 4: Expression levels of steroidogenic enzymes involved in aldosterone biosynthesis in wild-type or mutant animals (n=33) for each of the following genes: *Sspo, Dguok, Hoxaas2, Clstn3, Atm, Tipin, Mapk6*. Values are relatively expressed to the housekeeping gene *Gapdh*.

Figure 5: Histological examination of the adrenal glands of wild-type animals and mutants for all four following genes: *Sspo, Dguok, Hoxaas2, Clstn3.*Cell count of CYP11B2 positively stained cells per standardized area in the adrenal cortex of wild-type and mutant animals to the total cell count per area (A). Representative immunohistochemical staining of the adrenal cortex of wild-type (B) and mutant (C) mice. Ratios of CYP11B2 positively stained cells to the total cell count in the outer (D), middle (E) and inner (F) area of the adrenal cortex of wild-type and mutant mice (*** for $P<0.001$).

Table 1

cohort	Sspo				Dguok				Hoxaas2				Clstn3			
	wt	mut	fold	p	wt	mut	fold	p	wt	mut	fold	p	wt	mut	fold	p
All (n=126)	351±120	405±132	1.15	<0.05	354±127	408±120	1.15	<0.05	350±119	413±132	1.18	<0.01	346±116	428±132	1.23	<0.001
Restricted (n=99)	349±107	426±128	1.22	<0.01	354±117	431±114	1.22	<0.01	346±106	436±126	1.26	<0.001	341±101	459±123	1.34	<0.0001

Table 2

Aldosterone to Renin Ratio (ARR)			
		mean ± sd (% of mean of wild-types)	p-value
Sspo	wt (n=24)	100 ± 43	<0.05
	mut (n=17)	142 ± 71	
Dguok	wt (n=27)	100 ± 49	=0.09
	mut (n=14)	130 ± 60	
Hoxaas2	wt (n=27)	100 ± 47	=0.10
	mut (n=14)	130 ± 65	
Clstn3	wt (n=26)	100 ± 46	=0.80
	mut (n=15)	96 ± 55	

Figure 1

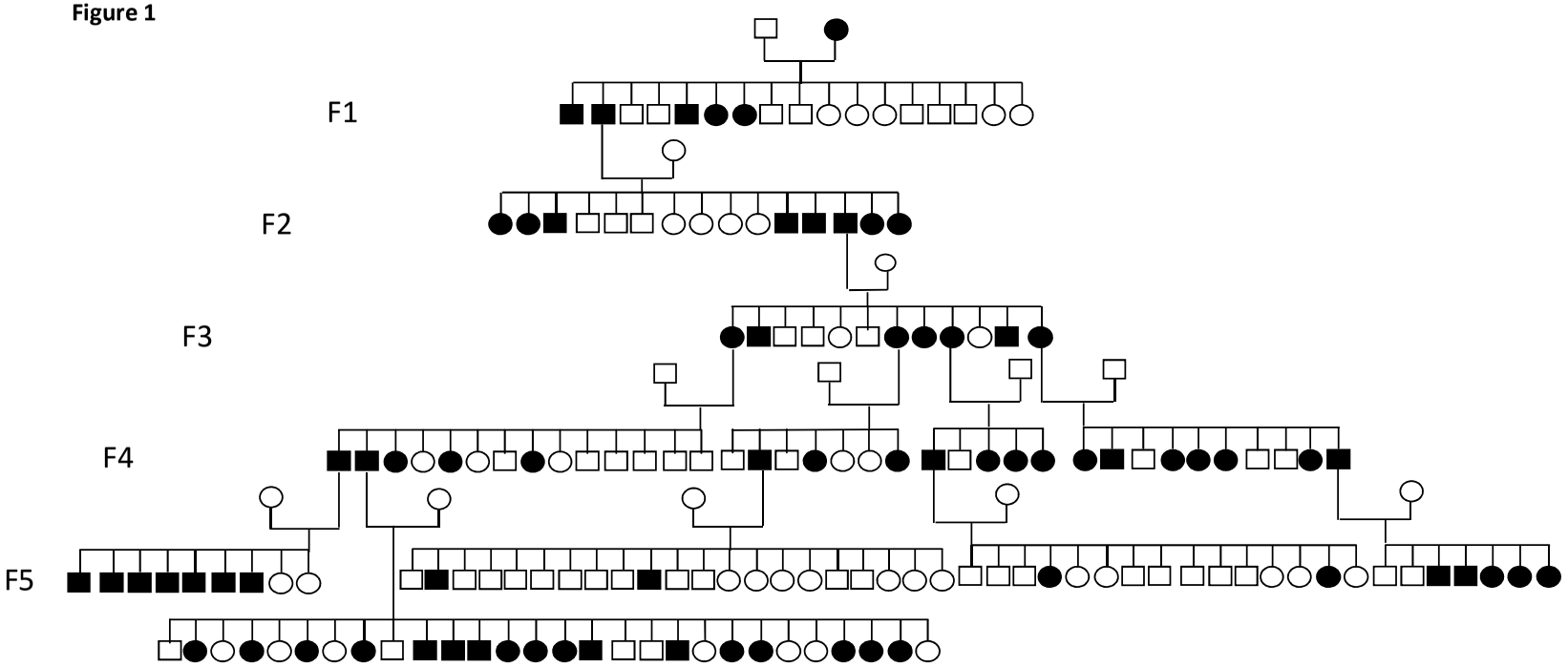

Figure 2

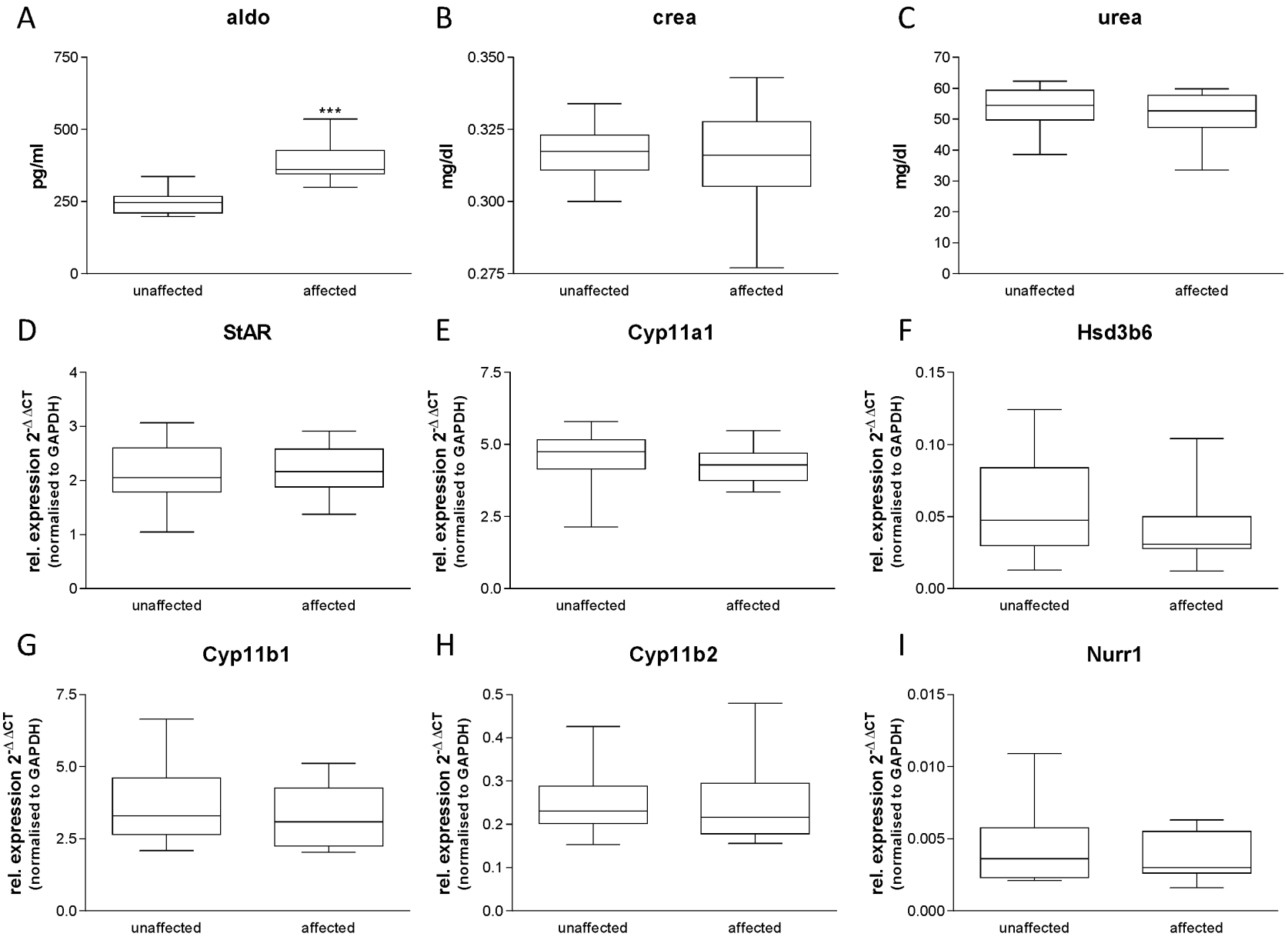
A
aldo
pg/ml
750
500
250
0
***
unaffected
affected
B
crea
mg/dl
0.350
0.325
0.300
0.275
unaffected
affected
C
urea
mg/dl
70
60
50
40
30
20
10
0
unaffected
affected
D
StAR
rel. expression 2-ΔΔCT (normalised to GAPDH)
4
3
2
1
0
unaffected
affected
E
Cyp11a1
rel. expression 2-ΔΔCT (normalised to GAPDH)
7.5
5.0
2.5
0.0
unaffected
affected
F
Hsd3b6
rel. expression 2-ΔΔCT (normalised to GAPDH)
0.15
0.10
0.05
0.00
unaffected
affected
G
Cyp11b1
rel. expression 2-ΔΔCT (normalised to GAPDH)
7.5
5.0
2.5
0.0
unaffected
affected
H
Cyp11b2
rel. expression 2-ΔΔCT (normalised to GAPDH)
0.5
0.4
0.3
0.2
0.1
0.0
unaffected
affected
I
Nurr1
rel. expression 2-ΔΔCT (normalised to GAPDH)
0.015
0.010
0.005
0.000
unaffected
affected

Figure 3

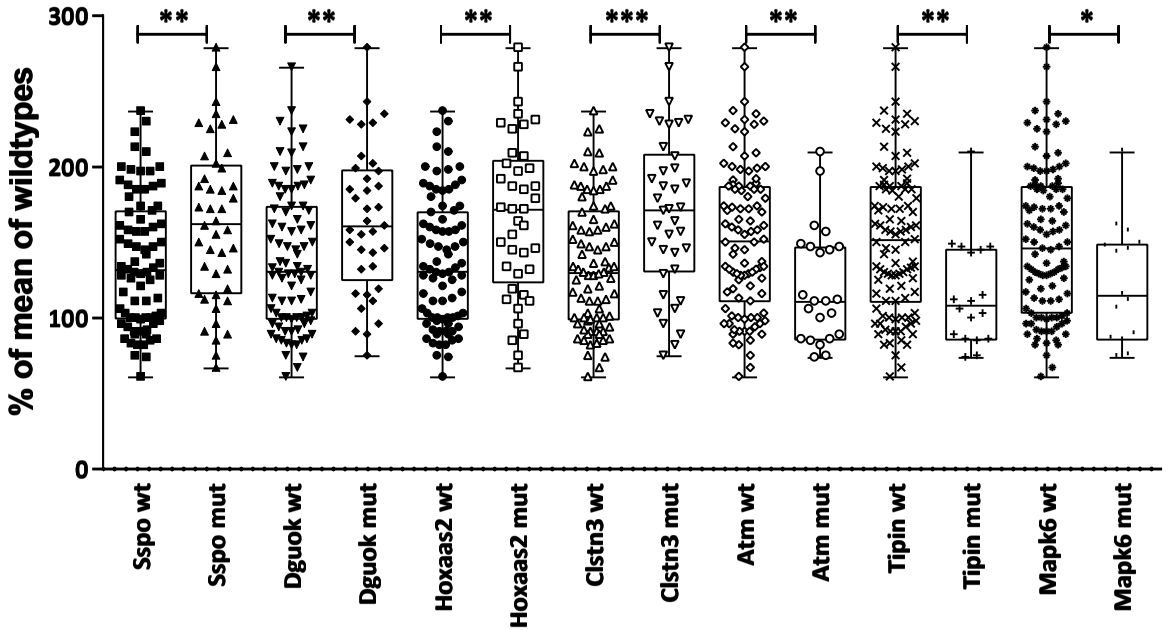
% of mean of wildtypes
300
200
100
0
**
**
**
***
**
**
*
Sspo wt
Sspo mut
Dguok wt
Dguok mut
Hoxaas2 wt
Hoxaas2 mut
Clstn3 wt
Clstn3 mut
Atm wt
Atm mut
Tipin wt
Tipin mut
Mapk6 wt
Mapk6 mut

Figure 4

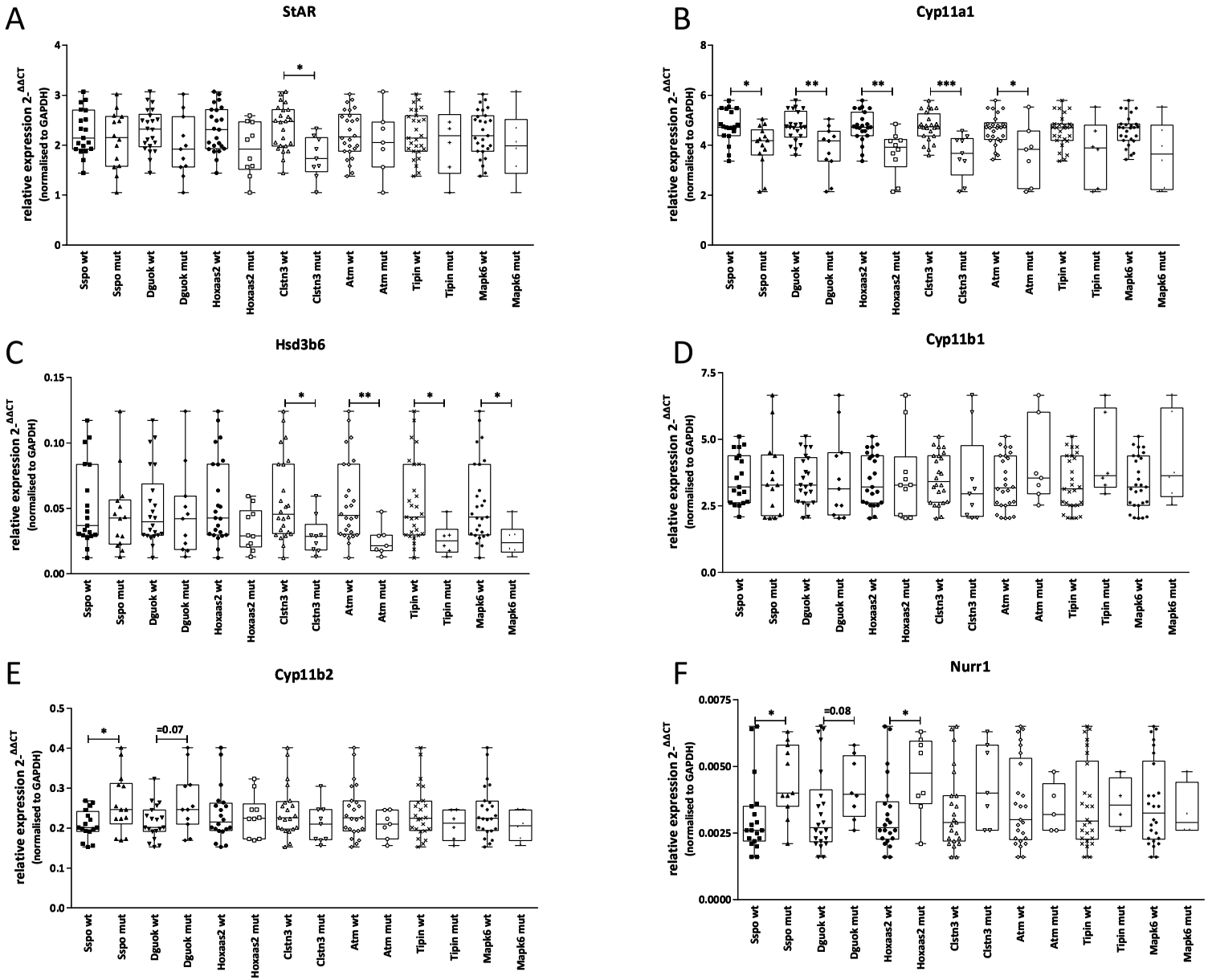
A
StAR
relative expression 2-ΔΔCT (normalised to GAPDH)
B
Cyp11a1
C
Hsd3b6
D
Cyp11b1
E
Cyp11b2
=0.07
F
Nurr1
=0.08
Sspo wt
Sspo mut
Dguok wt
Dguok mut
Hoxaas2 wt
Hoxaas2 mut
Clstn3 wt
Clstn3 mut
Atm wt
Atm mut
Tipin wt
Tipin mut
Mapk6 wt
Mapk6 mut

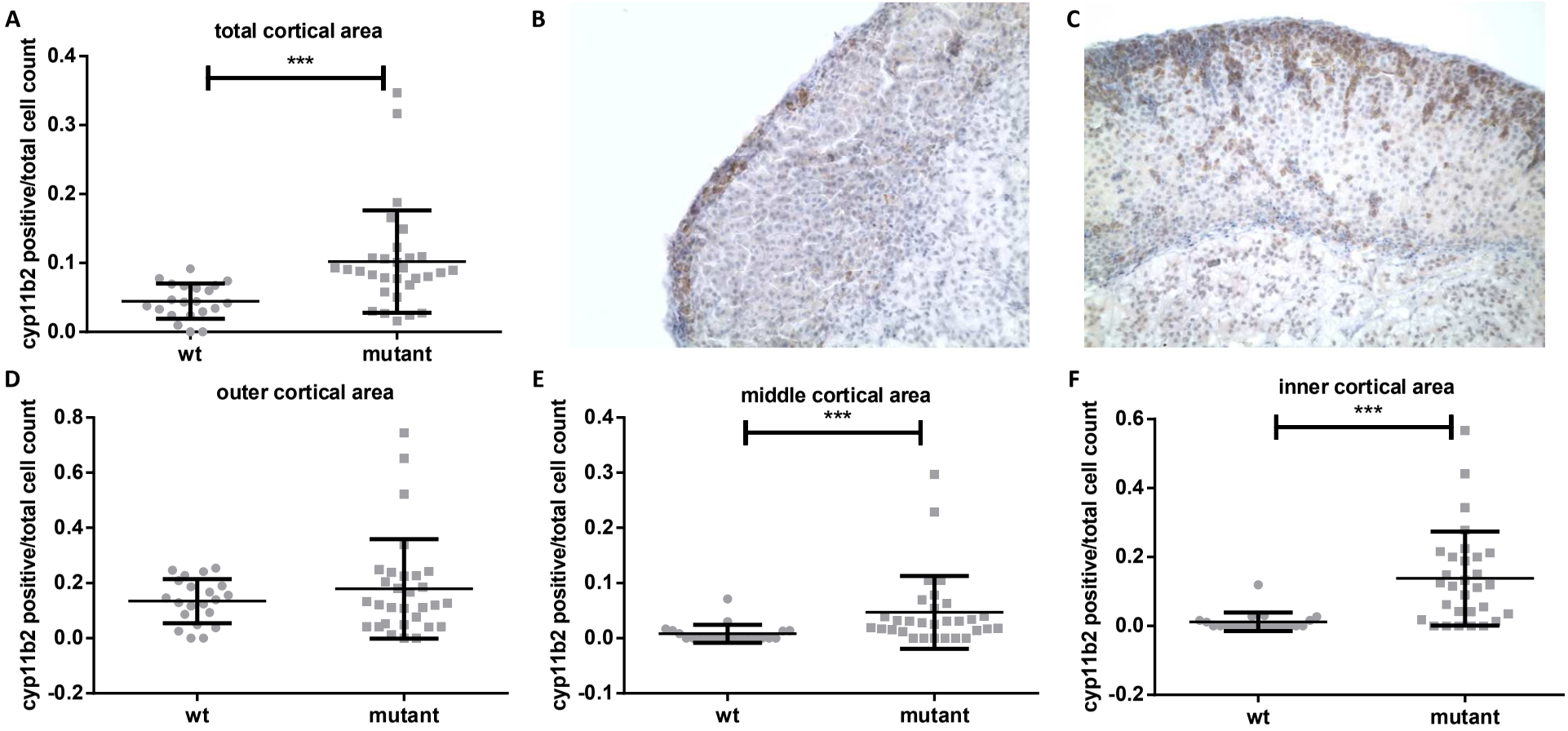
A
total cortical area
***
cyp11b2 positive/total cell count
0.4
0.3
0.2
0.1
0.0
wt
mutant
B
C
D
outer cortical area
cyp11b2 positive/total cell count
0.8
0.6
0.4
0.2
0.0
-0.2
wt
mutant
E
middle cortical area
***
cyp11b2 positive/total cell count
0.4
0.3
0.2
0.1
0.0
-0.1
wt
mutant
F
inner cortical area
***
cyp11b2 positive/total cell count
0.6
0.4
0.2
0.0
-0.2
wt
mutant